Case Study

Modeling of AOCS equipments of a LEO satellite

Version 1.7

1 Objective

The objective of the case study is to produce a functional simulation of some equipment involved in the AOCS system of a spacecraft in the early stage of the mission and from the computer driving the position of the spacecraft.

The simulation will be based on the SimTG Simulation Modeling Framework and developed in C++.

The following will provide a minimal description of the physical phenomena to be simulated and the AOCS equipment involved. The students are free to go beyond this description to add more complexity and/or representativity to their simulation.

The case study is intended for a group of two students.

2 Acronyms

Acronym	Meaning
AOCS	Attitude & Orbit Control System
ASH	Acquisition & Safe Hold
CSS	Coarse Sun Sensor
CSW	Central software (complete)
FOV	Field-of-view
FSM	Finite State Machine
FSW	Flight software (restricted to AOCS)
MAG	Magnetometer
MAN	Manoeuvrer
MTQ	Magneto-torquer
NM	Normal Mode
S/C	Spacecraft
SA	Solar arrays
TC	Telecommand
wrt	With respect to

3 Context

The AOCS flight software is a subpart of the complete central software dealing with the spacecraft attitude and orbit.

This case study focuses on the ASH mode, the NM and MAN mode will not be covered.

Just after the S/C is separated from the launcher last stage, the ASH is the first mode to run. Its mission is to place the S/C in a definite and secure configuration until the ground operator decide to switch to NM which is the nominal mission mode. ASH mode also acts as a last resort move if the FSW get trapped in a situation it cannot handle on its own (critical failure of a equipment, SW error, etc), the S/C will then remain in ASH until the ground operators can set up a restoration procedure.

In our case study the ASH shall ensure that:

1. the S/C angular rate will be aligned along one of the S/C main inertia axis in order to give it a gyroscopic stiffness,
2. the SA will be turned toward the Sun in order not to deplete the embedded batteries,

The second point is obviously critical since if the batteries was depleted, the FSW could no longer be run. Moreover, the thermal control will be interrupted, which may damage some devices beyond repair, leading to a partial or complete failure of the mission.

4 Spacecraft description

The considered S/C is a typical observation satellite orbiting around the Earth on a sun synchronous orbit. In the frame of our study, we will limit ourselves to the following devices:

- the sun sensor,
- the controller of the AOCS.

The S/C main body is modelled as a rigid body (no modal deformations). The frame R_s (X_s, Y_s, Z_s) is attached to the main body.

5 Sun Sensor

5.1 Functional description

The chosen sun sensor is the BASS.

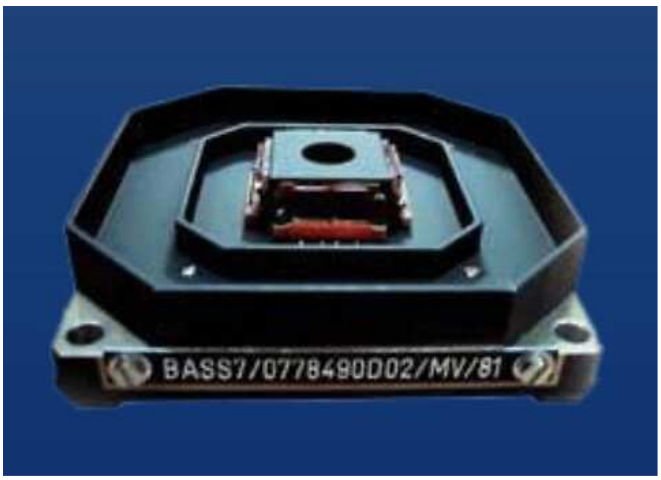

The sensor used the photo-electric effect to produce output currents.

The input Sun direction is given in the S/C frame. To the sensor is also given the eclipse status of the S/C. The boolean *e* will provide this data.

One needs to take into account two configuration parameters:

1. the mounting orientation of the CSS wrt the S/C,
2. the presence of a baffle, necessary to shield the sensor from stray light reflecting on the SA.

Thus the following inner flow-chart:

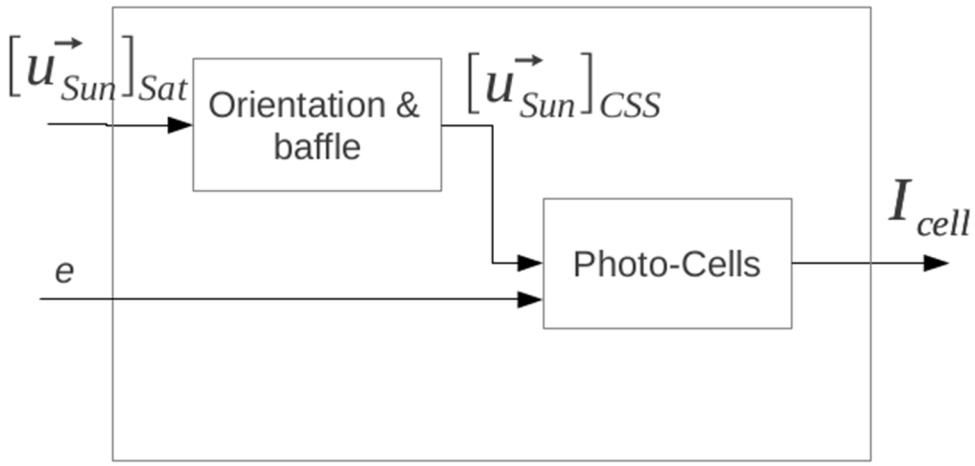

5.2 Orientation

The following frames are defined:

- R_s (X_s, Y_s, Z_s) the S/C frame,
- R_c (X_c, Y_c, Z_c) the CSS frame where X_c is the sensor neutral axis.

The frames relative orientation is defined by the change-of-basis matrix:

$[\vec{u}]_{CSS} = M_{Sat \Rightarrow CSS}[\vec{u}]_{Sat}$

With $\vec{u} \in \mathbb{R}^3$and $M_{Sat \Rightarrow CSS} \in \mathbb{R}^3 \times \mathbb{R}^3$.

The CSS is nominally mounted in such a way that X_c is along -Z_s, Y_c along +Y_s and Z_c along +X_s.

5.3 Convention

There is many ways to define the direction of the Sun in the CSS frame. The set of coordinates of the vector $\vec{u}_{sun}$ is one of them, but its geometric interpretation might not be easy. Thus we also define the orientation of the Sun as a couple of two angles:

- the co-elevation $\theta \in [0, \pi]$

- the azimuth $A_z \in [0,2\pi]$

The co-elevation is the angle separating the CSS X_c axis from the sun direction. When this angle is nil, the Sun is at the zenith of the CSS, when it is π, the Sun is at the nadir of the CSS.

The azimuth is the angle separating the CSS Z_c axis from the projection of the sun direction on the (Y_c, Z_c) plane. The azimuth is measured counter-clockwise, as shown in the figure below:

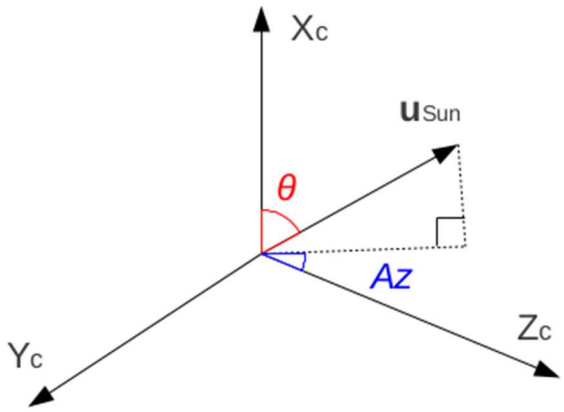

5.4 Baffle

These sensors are generally equipped with mission-specific baffles to avoid reflections from spacecraft parts having a negative effect on the measurement accuracy.

The baffle is to take into account physical limitation in the CSS field-of-view. It can be modelled as a black wall surrounding the CSS in order to protect it from stray light. The baffle effect can be illustrated as follows:

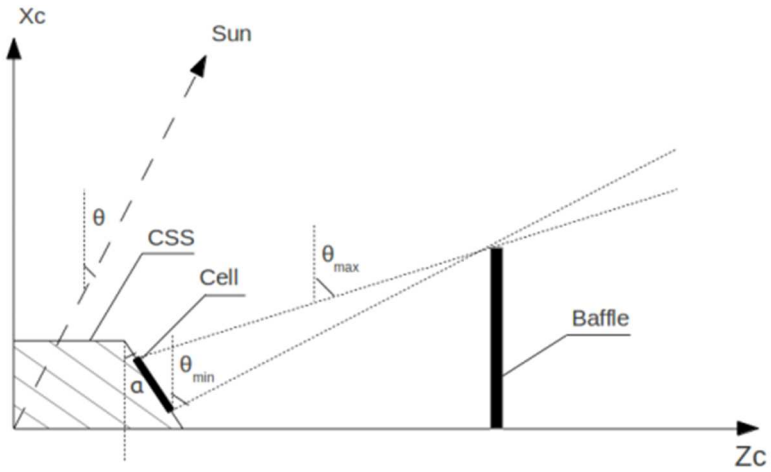

The wall is placed at a definite distance from the cell, blinding it when the Sun goes below the wall horizon. The effect of the baffle on the output current can be approximated by a coefficient *k* such as:

- $\theta < \theta_{min} \Rightarrow k = 1$
- $\theta_{min} \leq \theta \leq \theta_{max} \Rightarrow k = \frac{\sin(\theta_{max} - \theta)}{\sin(\theta_{max} - \theta_{min})}$
- $\theta > \theta_{max} \Rightarrow k = 0$

The values of the limit co-elevation angles depends on the baffle geometry and are functions of the Sun azimuth in the CSS frame. Moreover, these angles are relative to the considered cell. The precise calculation of the limit angles extracted from a particular geometry being a tedious task, the baffle is approximated by a set of 40 azimuthal sectors of 9 degrees centred on the CSS axis and the bisecting lines of the Y_c and Z_c axis:

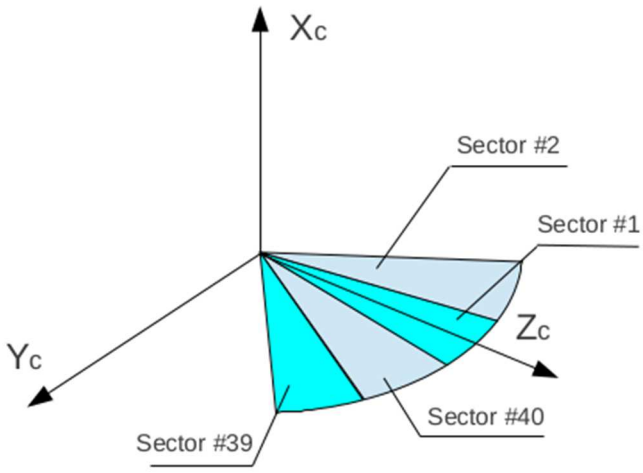

Note that the first sector begin at Azimuth 355.5° and end at Azimuth 4.5°. The cells are numbered counter-clockwise.

The values of the limit angles by sector by cells and some diagrams are given in annex.

5.5 Cell

The photo-electric cell has not a linear response curve, especially when the incident light is away from the normal to the cell.

The output current might be modelled as follows (for a particular cell):

$$I_{cell} = I_{max} \times (\vec{n} \cdot \vec{u}_{Sun} \times \lambda \times k \times e) + N(t)$$

with

$$\lambda = 1 - (\frac{2}{\pi} \times \arccos(\vec{n} \cdot \vec{u}_{sun}))^{\nu}$$

and

- I_{max} is the maximal current the cell delivers for a Sun at the cell zenith.
- $\vec{n}$ is a unit vector normal to the cell.
- ν is the large incident coefficient modelling the non-linearity of the cell.
- e is the eclipse status (0 if satellite is in the Earth shadow)

A white noise *N(t)* will also be added to the output. It is bound by the constant N_{CSS} and its value is randomly varying during the time.

The sensor is composed of 4 cells along the +/-Z_c and +/-Y_c axis. The cells are tilted from the vertical (X_c axis) by an angle of 22°.

6 Controller System

The spacecraft is equipped of propulsion to perform a rotation around Y_s and Z_s axis. The controller systems aims to rotate the spacecraft until reaching a position with maximal exposition of the solar panels. As the CSS is parallel panels, the optimal position is when all CSS cells are exposed with the same value. This means (a) that the rotation around Z_s is proportional to I_{Y+} - I_{Y-} (in the plane (X_s, Y_s)) and (b) that the rotation around Y_s is proportional to I_{Z+} - I_{Z-} (in the plane (X_s, Y_s)).

For the sake of simplicity, the controller system and the spacecraft are only represented by a single model producing the $\vec{u}_{sun}$vector. The effect of the propulsion units is to rotate this vector by some angle$\alpha_Y$and α_Z (which are limited to 10° per time unit). To sum up, the control system has to use the difference in the input current (I_{Y+}, I_{Y-}, I_{Z+}, I_{Z-}), to produce rotation angles and to use these angles to rotation the vector$\vec{u}_{sun}$. Maybe, a PID approach is a good solution to implement the controller system.

7 Numerical values

The following tables gathers numerical values to be considered in the case study.

Symbol	Description	Value	Unit
I_{max}	CSS max current	31e-3	A
ν	CSS exponent of the large incidence coefficient	9.6	-
N_{CSS}	CSS white noise amplitude	2.3e-10	A

8 Baffle definition

The CSS baffle definition is to be considered (angles are expressed in degrees in the CSS frame):

Sector	Z+ θ_{min}	Z+ θ_{max}	Y- θ_{min}	Y- θ_{max}	Z- θ_{min}	Z- θ_{max}	Y+ θ_{min}	Y+ θ_{max}
1	75.275	89.279	77.263	87.318	21.982	21.982	77.263	87.318
2	75.450	89.289	77.418	89.642	22.233	22.233	68.965	69.021
3	75.968	89.315	77.871	89.655	23.005	23.005	52.764	52.764
4	76.822	89.360	78.615	89.660	24.384	24.384	41.770	41.770
5	77.998	89.417	79.638	89.577	26.539	26.539	34.553	34.553
6	79.474	89.490	79.474	89.490	29.761	29.761	29.761	29.761
7	79.638	89.577	77.998	89.417	34.553	34.553	26.539	26.539
8	78.615	89.660	76.822	89.360	41.770	41.770	24.384	24.384
9	77.871	89.655	75.968	89.315	52.764	52.764	23.005	23.005
10	77.418	89.642	75.450	89.289	68.965	69.021	22.233	22.233
11	77.264	87.060	75.276	89.279	77.264	87.060	21.984	21.984
12	68.965	69.021	75.450	89.289	77.418	89.642	22.233	22.233
13	52.764	52.764	75.968	89.315	77.871	89.655	23.005	23.005
14	41.770	41.770	76.822	89.360	75.805	89.651	24.384	24.384
15	34.553	34.553	77.998	89.417	71.582	89.565	26.539	26.539
16	29.761	29.761	77.590	89.490	68.167	81.939	29.761	29.761
17	26.539	26.539	68.482	89.577	65.371	76.850	34.553	34.553
18	24.384	24.384	66.528	87.162	63.210	75.570	41.770	41.770
19	23.005	23.005	65.130	82.122	61.676	74.642	52.764	52.764
20	22.233	22.233	64.295	81.822	60.759	74.081	63.686	69.021
21	21.984	21.984	64.016	81.550	60.456	73.892	64.016	81.550
22	22.233	22.233	63.686	69.021	60.759	74.081	64.295	81.822
23	23.005	23.005	52.764	52.764	61.676	74.642	65.130	82.122
24	24.384	24.384	41.770	41.770	63.210	75.570	66.528	87.162
25	26.539	26.539	34.553	34.553	65.371	76.850	68.482	89.577
26	29.761	29.761	29.761	29.761	68.167	81.939	77.590	89.490
27	34.553	34.553	26.539	26.539	71.582	89.565	77.998	89.417
28	41.770	41.770	24.384	24.384	75.805	89.651	76.822	89.360
29	52.764	52.764	23.005	23.005	77.871	89.655	75.968	89.315
30	68.965	69.021	22.233	22.233	77.418	89.642	75.450	89.289
31	77.264	87.060	21.984	21.984	77.264	87.060	75.276	89.279
32	77.418	89.642	22.233	22.233	68.965	69.021	75.450	89.289
33	77.871	89.655	23.005	23.005	52.764	52.764	75.968	89.315
34	78.615	89.660	24.384	24.384	41.770	41.770	76.822	89.360
35	79.638	89.577	26.539	26.539	34.553	34.553	77.998	89.417
36	79.474	89.490	29.761	29.761	29.761	29.761	79.474	89.490
37	77.998	89.417	34.553	34.553	26.539	26.539	79.638	89.577
38	76.822	89.360	41.770	41.770	24.384	24.384	78.615	89.660
39	75.968	89.315	52.764	52.764	23.005	23.005	77.871	89.655
40	75.450	89.289	68.965	69.021	22.233	22.233	77.418	89.642

The following graphics show the influence of baffle on the field-of-view limitation for each cell. The radial axis is the co-elevation of the Sun in the CSS frame, the angular axis its azimuth. Note that if seen from above, the $+Z_c$ axis would be at Az = 0, and the $+Y_c$ axis at Az =270°.

For co-elevations inside the green curve (min) there is no obstacle between the Sun and the cell (k = 1). For co-elevations outside the red curve (max) the Sun is completely hidden from the cell (k = 0). Between the two curves, the coefficient k is decreasing (from min to max).

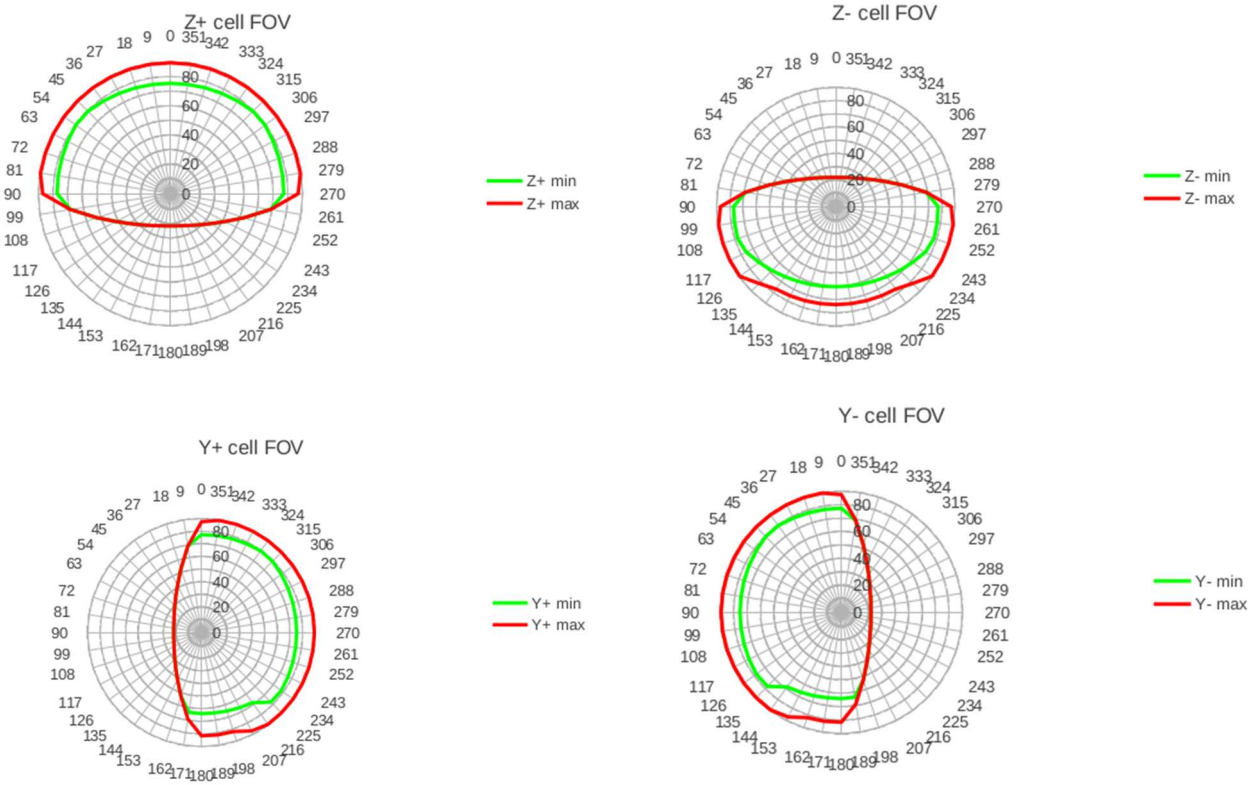

These diagrams show that the CSS FOV is reduced in the -Z direction (due to a cache to hide a white antenna). Note that the CSS will provide the maximum of information if the co-elevation of the Sun is lower than the tilt-angle of the cells, because all the cells will be able to measure the Sun direction at the same time.